ISSN 0208-7774 TRIBOLOGIA 1/2023 p. 19–26
DOI: 10.5604/01.3001.0016.2930

Henryk BĄKOWSKI[*], Janusz CEBULSKI[**], Janusz ĆWIEK[***]

EVALUATION OF THE WEAR OF AN FE-AL ALLOY TURBOCHARGER ROTOR SEAL RING UNDER SELECTED OPERATING CONDITIONS

OCENA ZUŻYCIA PIERŚCIENIA USZCZELNIAJĄCEGO WIRNIKA TURBOSPRĘŻARKI WYKONANEGO ZE STOPU FE-AL W WYBRANYCH WARUNKACH EKSPLOATACJI

Key words: wear abrasive, turbocharger rotor seal ring, Fe-Al alloy.

Abstract: This publication presents the possibility of extending the service life of the rotor shaft seal ring in an automotive turbocharger by using an intermetallic Al-Fe alloy. Comprehensive results of tribological, metallographic and profilometric tests of this alloy (vacuum cast) operating in a sliding association on a T-05 bench allowed the representation of a real friction node. Based on empirical tests, it will be possible to determine which alloy (Al-Fe alloy or the one currently used for sealing rings of a car turbocharger rotor shaft) has better tribological properties. For this purpose, the research was based on an experiment that assumes three main factors determining the wear of the tested association. The result of the experimental plan was to obtain three-dimensional diagrams showing the influence of the wear factors on the friction force and surface topography.

Słowa kluczowe: zużywanie ścierne, pierścień uszczelniający wirnika turbosprężarki, stop Fe-Al.

Streszczenie: W publikacji przedstawiono możliwość wydłużenia czasu eksploatacji pierścienia uszczelniającego wałka wirnika w turbosprężarce samochodowej poprzez zastosowanie międzymetalicznego stopu Al-Fe. Kompleksowe wyniki badań tribologicznych, metalograficznych oraz profilometrycznych tego stopu (odlewanego próżniowo) pracującego w skojarzeniu ślizgowym na stanowisku T-05 pozwoliły na odzwierciedlenie rzeczywistego węzła tarcia. Na podstawie przeprowadzonych badań empirycznych będzie można stwierdzić, który ze stopów (stop Al-Fe czy obecnie stosowany na pierścienie uszczelniające wałka wirnika turbosprężarki samochodowej) posiada lepsze właściwości tribologiczne. W tym celu badania oparto na eksperymencie, który zakłada trzy główne czynniki decydujące o zużyciu badanego skojarzenia. W wyniku przeprowadzonego planu eksperymentu możliwe było uzyskanie wykresów trójwymiarowych ujmujących wpływ czynników eksploatacyjnych na siłę tarcia oraz topografię powierzchni.

INTRODUCTION

Currently, diesel and petrol engines are still being fitted with supercharging, mainly because road transport is based on vehicles equipped with this engine power supply. However, the approach to spark-ignition engines has changed. Nowadays, in a world of "downsizing", dynamic and powerful engines are obtained from a very small engine volume and are powerful through turbochargers. In order to illustrate the technological progress that has been made in recent years, it is enough to compare the ratio of engine power generated to engine capacity from the early 1990s versus the

[*] ORCID: 0000-0002-9041-1991. Silesian University of Technology, Faculty of Transport and Aviation Engineering, Z. Krasińskiego 8 Street, 40-019 Katowice, Poland.
[**] ORCID: 0000-0002-3813-8705. Silesian University of Technology, Faculty of Materials Engineering, Z. Krasińskiego 8 Street, 40-019 Katowice, Poland.
[***] ORCID: 0000-0003-1829-2067. Silesian University of Technology, Faculty of Transport and Aviation Engineering, Z. Krasińskiego 8 Street, 40-019 Katowice, Poland.

modern period. It is easy to see that in the 1990s, the engine power of 73.55 kW was derived from a displacement of 2000 cc; today, it is only 1000 cc. Older engines derive power from capacity; in newer designs, obtaining such power from such a small capacity is impossible. Due to the turbochargers' role in the supercharging process, proper operation of the turbocharger will help avoid breakdowns and costly repairs. A turbocharger consists of a combustion turbine and a compressor mounted on a common shaft. In order to drive the turbocharger, the kinetic energy of the exhaust gas is used, as the exhaust gas contains about 30 per cent of the energy generated by the combustion of the fuel-air mixture. These exhaust gases are able to drive the turbocharger's rotor at 100000 to 200000 revolutions per minute. Such an accelerated rotor triggers the turbocharger. The seal ring is the critical point most exposed to wear **[L. 2]**.

Typical oil seals (O-rings) cannot be used to build turbocharger seals. However, the construction of a turbocharger seal system is quite simple. On both the air side and the turbine side, a so-called oil reject works together with a sealing ring and

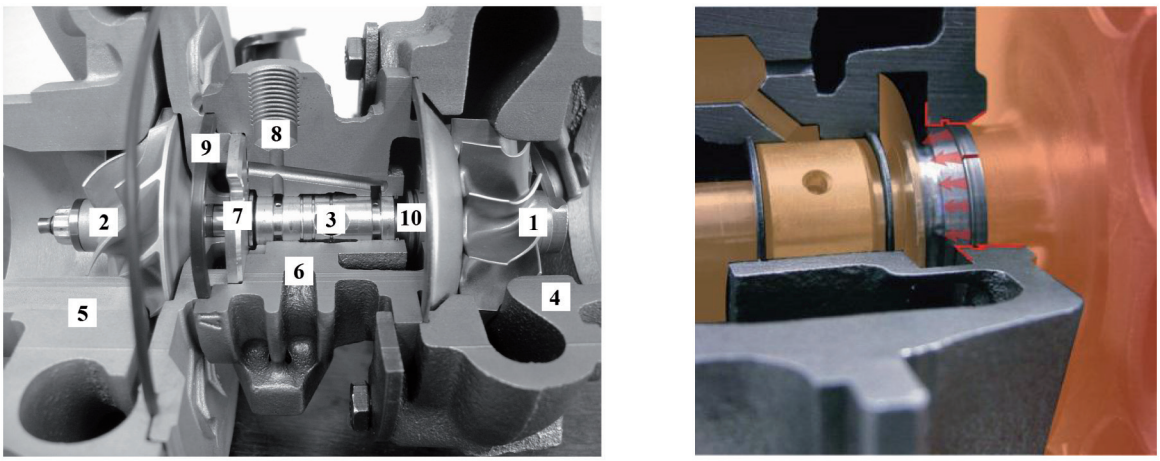

a) b)

Fig. 1. Construction of turbocharger: a) cross section; 1 – turbine rotor, 2 – compressor rotor, 3 – slide bearing, 4 – turbine housing, 5 – compressor housing, 6 – central housing, 7 – thrust bearing, 8 – oil channel, 9 – sealing ring, 10 – shaft; a) working principle of sealing ring, b) friction node analysed [L. 1]

Rys. 1. Budowa turbosprężarki: a) przekrój poprzeczny; 1 – wirnik turbiny, 2 – wirnik sprężarki, 3 – łożysko ślizgowe, 4 – obudowa turbiny, 5 – obudowa sprężarki, 6 – obudowa centralna, 7 – łożysko oporowe, 8 – kanał olejowy, 9 – pierścień uszczelniający, 10 – wał; a) zasada działania pierścienia uszczelniającego, b) analizowany węzeł tarcia **[L. 1]**

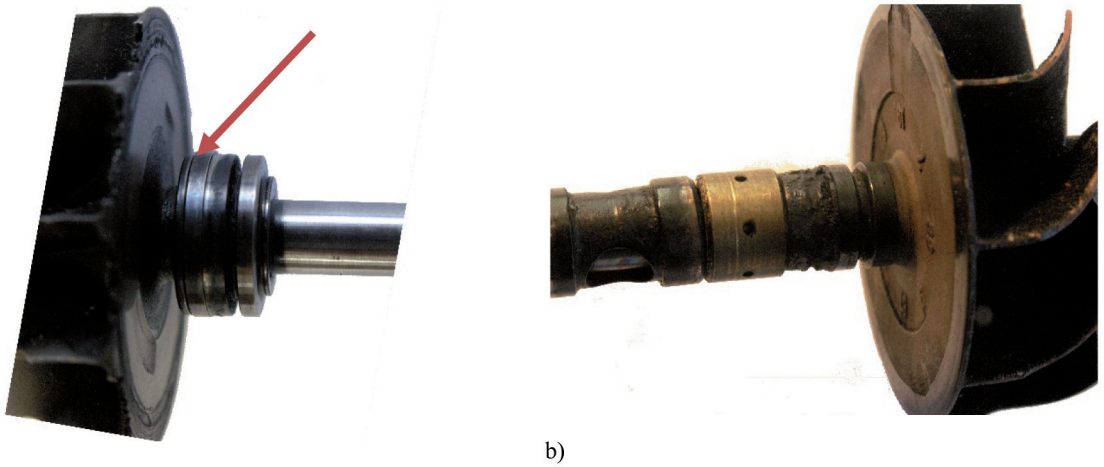

a) b)

Fig. 2. Wear of sealing ring and shaft groove on turbines: a) permissible wear, b) excessive wear (red arrow marks the location of the sealing ring)

Rys. 2. Zużycie pierścienia uszczelniającego i rowka na wałku turbin: a) zużycie dopuszczalne, b) nadmierne zużycie (czerwoną strzałką zaznaczono lokalizację pierścienia uszczelniającego)

only during the rotation of the turbocharger shaft does the centrifugal force reject oil outwards into special oil spaces, which flows by gravity into the oil sump. The fitted steel sealing ring (**Fig. 2a**) pressed down by exhaust gas pressure further seals the system. Exactly the same phenomenon can be observed on the air side; the only difference is in the construction of the oil rejector, which is built into a so-called back plate or is an entirely separate component. Seals made of elastomers cannot be used in the system due to the high temperature, and mechanical seals in the form of specially made metal O-rings with a high content of heat-resistant materials such as nickel or chromium must be used. The seals only reach their full efficiency when under load, therefore any irregularities in the design result in sucking the engine oil into the working environment of the turbine (which causes its mineralisation, loss of lubricating properties, increase in resistance to motion, and as a result – an increase in temperature and risk of seizure of the turbocharger) or into the working environment of the compressor (which is relatively much more dangerous, as it may lead to a runaway engine). and a risk of turbocharger seizure) or to the compressor's working environment (which is relatively much more dangerous, as it may lead to a runaway compression-ignition engine). The diesel spray causes this by the compressor through the intercooler in the combustion chamber. This results in the combustion of diesel fuel which is not designed for a similar function (when the long chains of synthetic oil are torn apart, a great deal of exhaust fumes are produced, with a characteristic white colour, which drives the turbocharger, increasing the amount of diesel fuel sprayed and consequently further increasing the speed of the turbocharger and the engine) and as a result can lead to serious damage when the turbocharger and the rotor speed it reaches lead to a loss of balance **[L. 3]**.

For these reasons, the authors of this publication have used, instead of a steel ring, a material with very good strength and stiffness at high temperatures, high resistance to the destructive effects of the aggressive environment and oxidation (corrosion) and dimensional stability **[L. 4, 5, 6]**. Fe-Al alloys are characterised by such features. The main disadvantage of these materials, which hinders their processing by conventional forming or cavity (machining) methods, is their low ductility at ambient temperature **[L. 7]**.

The study aimed to determine the frictional resistance of the analysed junction in the presence of a lubricant (engine oil 5W 40), as well as the influence of operating conditions on the topography of the friction surface, which results in the tightness of the coupled.

MATERIALS AND TEST PROCEDURE

A cast iron called Niresist is used for turbocharger blocks, which contains 11÷16 % Ni, 2.5 % Si, up to 2.0 % Mn, up to 4.0 % Cr and up to 8.0 % Cu – it is characterised by high heat, wear and corrosion resistance. Aluminium alloys are also used for compressor bodies. Turbine rotors are manufactured from alloys called Inconel, MarM247 or titanium alloy. Inconel – i.e., an alloy of nickel, chromium, cobalt and iron with a nickel content of 46÷65%. The MarM247 alloy has 19% Cr, 9.0% Fe, 5.0% Nb, 3.0% Mo, 0.9% Ti, 0.6% Al and 0.05% C. The above alloys are characterised by high corrosion resistance at high temperatures. For turbocharger shafts, chromium-nickel-tungsten steels are used, i.e., structural alloy steels for quenching and tempering 25H2NWA containing 0.25% C, 0.4% Mn, 1.5% Cr, 4.2% Ni and 1.0% W. For the turbocharger's plain bearings, bronze casting alloy B102 (CuSnZn2) is used, characterised by high temperature and wear resistance. Heat-resistant materials with high chromium and nickel contents are used for sealing rings **[L. 8, 9]**. In this paper, the authors proposed alloys on the Fe-Al intermetallic phase matrix with an aluminium content of 40% (**Fig. 3**).

Analysing the results of the work **[L. 10]** on the heat resistance of the intermetallic alloy, it can be assumed that the corrosion product is the Al_2O_3 compound. The oxygen present on the friction surface is associated with the formation of a passive Al_2O_3 layer, providing high corrosion resistance. The addition of molybdenum increases the incandescence in Fe-Al alloys, as it leads to an increase in the transformation temperature of DO_3 in the phase with B2 crystalline structure, resulting in an increase in the energy of the antiphase boundary and also inhibits the diffusion of aluminium. Increasing the aluminium content in the alloy results in an increase in strength properties but with a decrease in ductility, while the addition of chromium results in a decrease in brittleness **[L. 11, 12]**. In works **[L. 13, 14]**, the authors show a number of advantages of Fe-Al alloys, corrosion

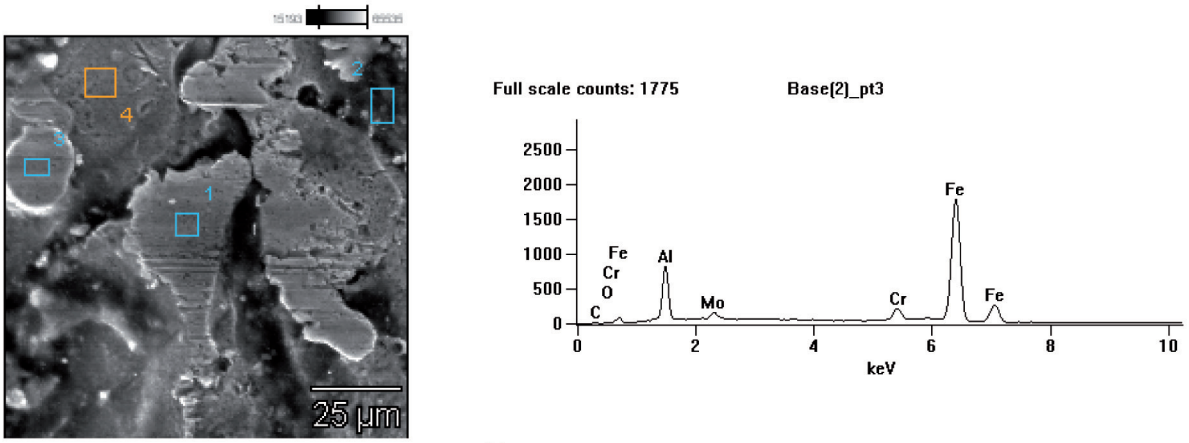

a) b)

Fig. 3. View of the friction surface of the Fe40Al5Cr0.2TiB intermetallic alloy (a) and X-ray microanalysis of the chemical composition of the tested surface

Rys. 3. Widok powierzchni tarcia stopu międzymetalicznego Fe40Al5Cr0,2TiB (a) oraz mikroanaliza rentgenowska składu chemicznego badanej powierzchni

resistance, good mechanical properties at elevated or high temperatures, or high wear resistance in aggressive environments. By using Fe-Al alloy powders, the problem of heterogeneity of chemical composition in the volume of the whole material is eliminated, and admixtures of elements such as Ti, Mo or Si definitely improve strength, while B, C or Zr positively improve the ductility of this material.

The Tribotester T-05 was used in tribological tests in a block-on-ring system (**Fig. 4a, c**). In this way, the shape of the mating surface of the sealing ring and the turbocharger rotor shaft was mapped.

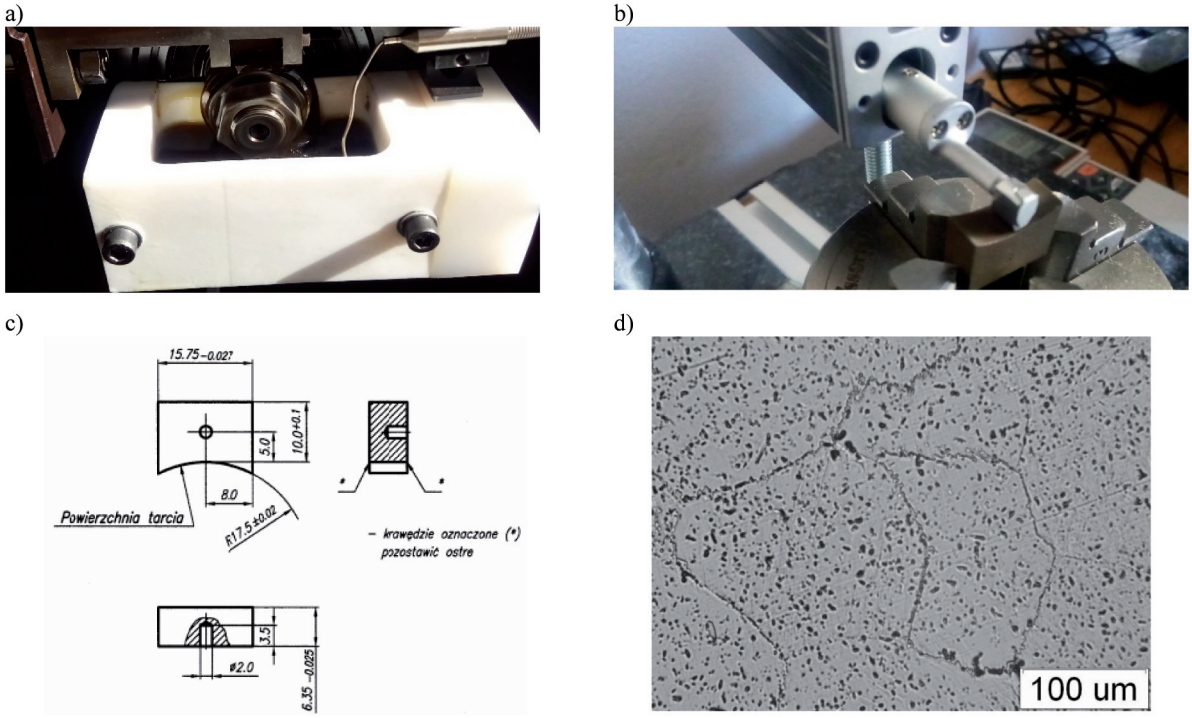

Fig. 4. View of a) a friction node on a T-05 stand, b) an example of a surface roughness measurement using a MITUTOYO touch profilometer, c) a drawing with the dimensions of the sample plotted, d) the microstructure of the intermetallic alloy Fe40Al15Cr0.2TiB

Rys. 4. Widok: a) węzła tarcia na stanowisku T-05, b) przykładowego pomiaru chropowatości powierzchni za pomocą profilometru dotykowego MITUTOYO, c) rysunku z naniesionymi wymiarami próbki, d) mikrostruktury stopu międzymetalicznego Fe40Al15Cr0,2TiB

The test conditions correspond to those of a real friction node (**Table 1**). Samples were cut using electrical discharge machining (WEDM) and subjected to tribological tests with three repetitions, while a tapered roller-bearing outer ring made of 100Cr6 bearing steel was used as a counter-example. The tests were performed based on a poliselective D-optimal experimental plan **[L. 15]**. The material used for the specimens mapping the cooperation surface of the turbocharger rotor sealing ring is single-phase, so it is not possible to indicate different phases (**Figure 4d**). The structure is type B2 at the atomic level, and this type of structure is fundamental from the point of view of wear resistance. Thus, the grain set structure is not a fundamental factor, as the material has a hardness of approx. 30 HV1.

The testing time of each individual sample was between 3–12 hours. For velocity 400 min^{-1}, it was 3 hours and 100 min^{-1} it was 12 hours, which was equivalent to 72000 cycles. During the tests, the friction force was measured using a strain gauge force sensor with an accuracy of 2.5% of the measured value and the weight loss of the samples using an AS220/C/2 analytical balance with an inaccuracy of 0.2 mg. The wear of the Fe-Al alloy surface was immeasurable.

The load was chosen to represent the pressure present in the exhaust system before the turbine. According to the work **[L. 16]**, the pressure varies between 0.1–0.3 MPa. The sample contact area is 100 mm^2, and the loading force Q is 10–30 N, respectively. The operating temperature of the tested pairing (20–140°C) is determined by the oil temperature under normal operating conditions of the internal combustion engine turbine (**Tab. 1**).

Table 1. Study plan according to the D-optimal poliselection sub-plan
Tabela 1. Plan badań zgodny z D-optymalnym poliselekcyjnym planem cząstkowym

Sample No.	Controlled factors on a standardised scale			Controlled factors on a real scale		
	$\hat{Q}$	$\hat{n}$	$\hat{t}$	Q, N	n, min^{-1}	t, °C
1	-1	+1	-1	10	400	20
2	+1	-1	-1	30	100	20
3	-1	-1	+1	10	100	140
4	+1	-1	+1	30	400	140
5	-1	0	0	10	250	80
6	+1	0	0	30	250	80
7	0	0	-1	20	250	20
8	0	0	+1	20	250	140
9	0	-1	0	20	100	80
10	0	+1	0	20	400	80
11	0	0	0	20	250	80

TEST RESULTS AND DISCUSSION

During the tests, friction forces were measured using a strain gauge force transmitter. The accuracy of the measuring track was 3% of the measured value. The working surfaces of the samples were subjected to profilometric tests after the tests. The test results are presented in **Table 2**.

Table 2. Summary of tribological test results
Tabela 2. Zestawienie wyników badań tribologicznych

No.	X_1	X_2	X_3	Roughness Rz [µm]	Standard deviation Rz [µm]	Max. friction force T [N]	Standard deviation T [N]
01	-1	-1	+1				
02	+1	-1	-1	15.738	0.092	4.48	0.15
03	-1	+1	-1	17.093	0.112	3.20	0.32
04	+1	+1	+1	17.251	0.171	6.97	0.23
05	-1	0	0	16.743	0.084	2.12	0.21
06	+1	0	0	17.961	0.129	6.94	0.23
07	0	-1	0	15.565	0.078	4.38	0.22
08	0	+1	0	17.571	0.023	3.36	0.17
09	0	0	-1	24.448	0.094	1.53	0.07
10	0	0	+1	16.284	0.008	6.37	0.31
11	0	0	0	17.318	0.076	3.85	0.19

The dependence of frictional force on load (Q), rotational speed (n) and temperature at the contact (t) is adequately described by equation 1. A graphical interpretation of the general equation (1) is shown in **Fig. 5**.

$$z = k_0 + k_{11}x_1^2 + k_{22}x_2^2 + k_{33}x_3^2 + k_{13}x_1x_3 + k_{12}x_1x_2 + k_{23}x_2x_3 \quad (1)$$

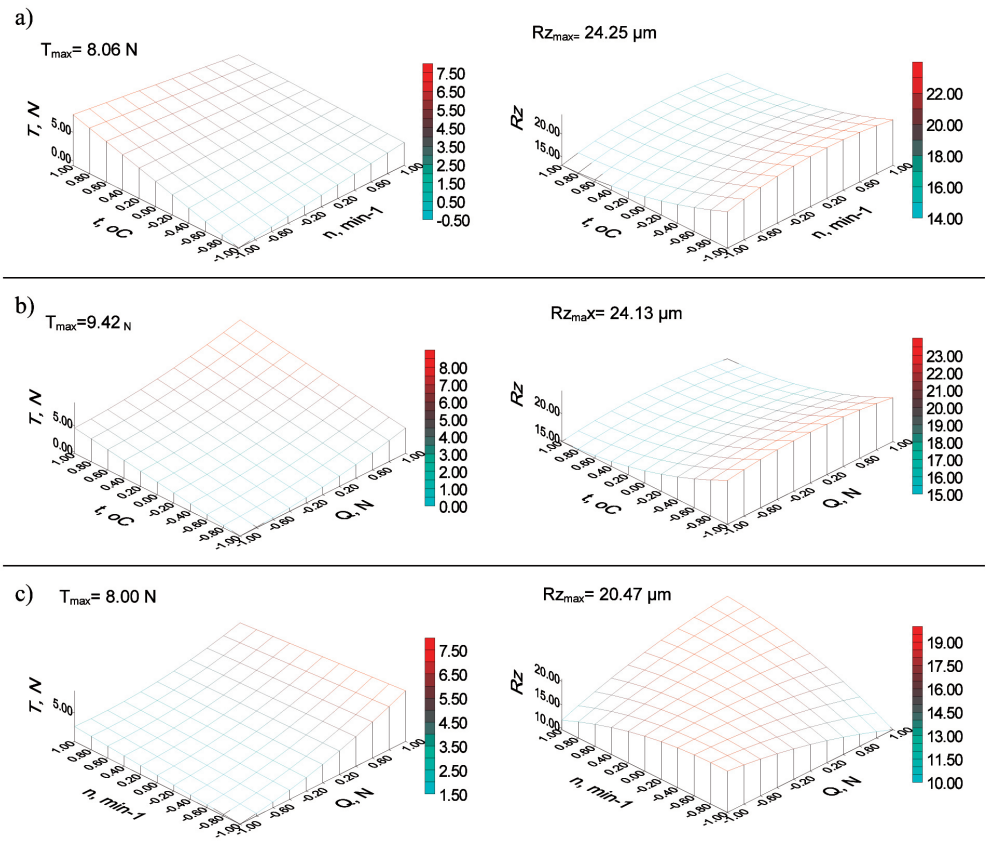

Fig. 5. Dependence of frictional resistance T and surface roughness Rz in a sliding contact after a tribological test equivalent to: a) centre load (0.2 MPa) under various speed and temperature conditions, b) centre line speed (250 min^{-1}) under various load and temperature conditions, c) centre temperature (80°C) under various load and speed conditions

Rys. 5. Zależność oporów tarcia T i chropowatości powierzchni Rz w skojarzeniu ślizgowym po teście tribologicznym odpowiadającemu: a) obciążeniu na poziomie centralnym (0,2 MPa) w różnych warunkach prędkości i temperatury, b) prędkości na poziomie centralnym (250 min^{-1}) w różnych warunkach obciążenia i temperatury, c) temperaturze na poziomie centralnym (80°C) w różnych warunkach obciążenia i prędkości

Based on the analysis of the results obtained, it can be concluded that the frictional force increases with increasing pressure and temperature. This is normal, as an increasing load on the friction node increases the actual contact area and increasing temperature in the association causes a slow loss of lubricating properties. The result is a transition from fluid friction to boundary friction. When considering the effect of velocity and temperature, surface roughness values decreased and increased with increasing load. This is related to the contacting of the tops of the roughness of the mating surfaces with decreasing speed and the smoothing of the friction surface (**Fig. 5**).

Profilometric tests also confirm the wear resistance of the used Fe-Al alloy. A slight increase in the value of the Rz parameter was observed after cooperation in the sliding contact, compared to the surface obtained directly after the machining (WEDM) (**Fig. 6**).

Metallographic tests were carried out on a Hitachi S-3400N scanning microscope and an Olympus C40 light microscope. The results are shown in **Fig. 6**.

Figure 7 shows images of the friction surface of a Fe-Al alloy after cooperation in sliding contact under laboratory conditions and of the surface of a sealing ring made of a conventional material

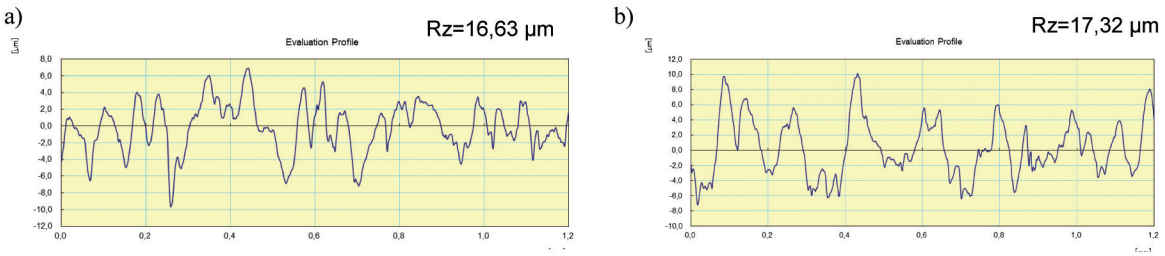

Fig. 6. Surface roughness profile of the Fe-Al alloy sample: a) after WEDM, b) after cooperation
Rys. 6. Profil chropowatości powierzchni próbki ze stopu Fe-Al: a) po obróbce elektroerozyjnej WEDM, b) po współpracy

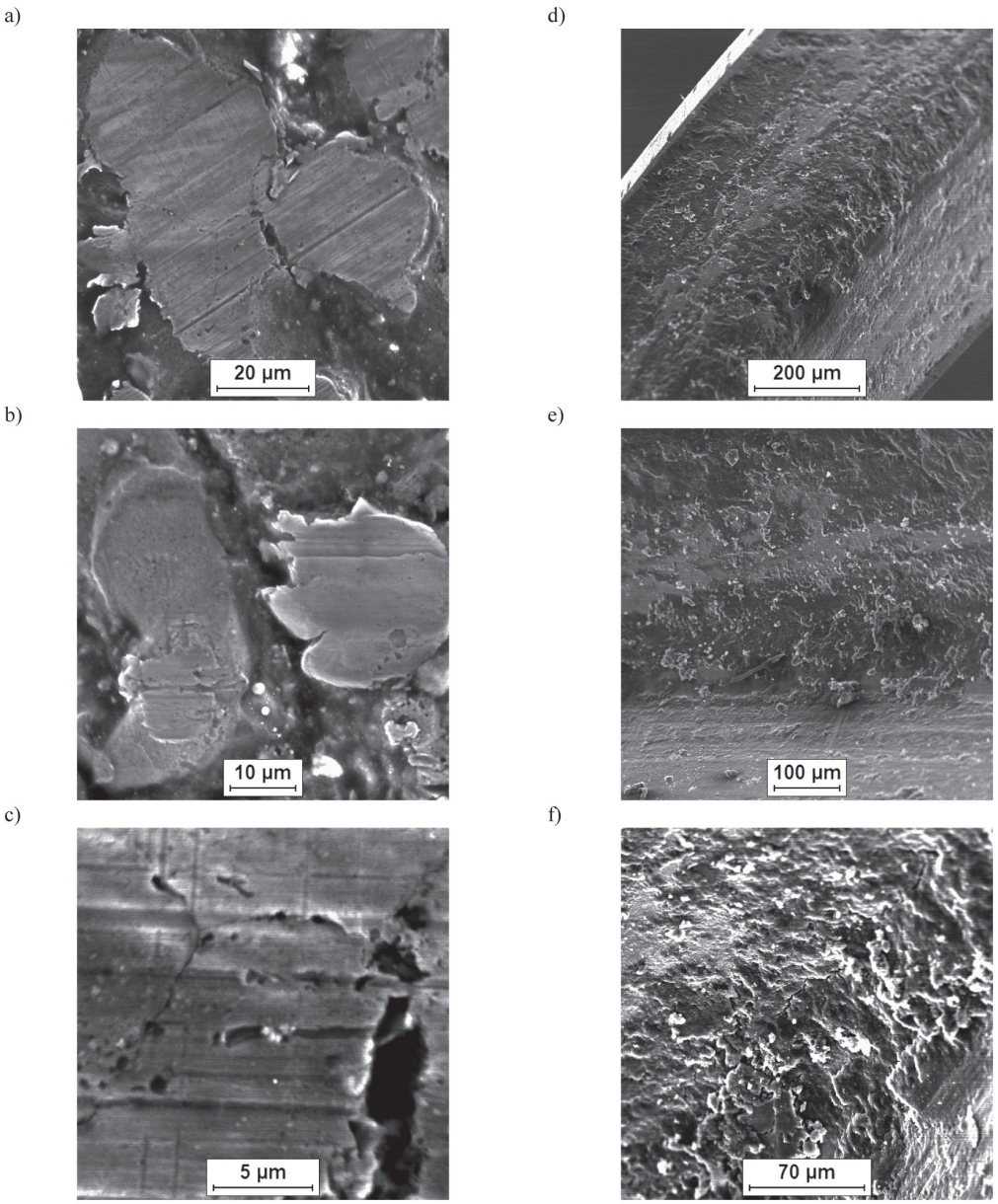

Fig. 7. Surface of the Fe-Al alloy specimen after cooperation (a, b, c) and the sealing ring from the real object (d, e, f)
Rys. 7. Powierzchnia próbki ze stopu Fe-Al po współpracy (a, b, c) oraz pierścienia uszczelniającego z obiektu rzeczywistego (d, e, f)

cooperating with a real object. In both cases, the mechanism is adhesive and abrasive wear, as evidenced by numerous scratches and flat areas of plastic deformation. However, on the sealing ring removed from the real object, numerous cracks can additionally be observed on the surface, which were not observed on the surface of the Fe-Al alloy. These cracks can lead to delamination (flake) wear, which leads to significant weight loss and, thus, dimensional deviations. Such a process results in a loss of leakage and oil penetration outside the lubrication circuit.

CONCLUSIONS

On the basis of the research carried out, it was found that:

- the dominant wear mechanism in the analysed combination is adhesive wear with accompanying abrasive wear,
- as the load and temperature of the lubricating medium increase, frictional resistance increases, while it decreases with increasing speed,
- the preliminary tests performed are very optimistic, as no cracks appeared on the Fe-Al alloy surface and the mass loss was immeasurable; therefore, it is necessary to make a sealing ring of Fe-Al alloy, which is then applied to the real object, i.e., a turbocharger of an internal combustion engine.

REFERENCES

1. Hadryś D., Bąkowski H., Stanik Z., Kubik A.: Analysis of shaft wear in turbocharges of automotive vehicles. Transport Problems, vol. 14, iss. 3, 2019, pp. 85–95.
2. Mysłowski J.: Doładowanie silników. Wydawnictwo Komunikacji i Łączności. Warszawa 2016.
3. Schweizer B., Sievert M.: Nonlinear oscillation of automotive turbocharger turbines. Journal of Sound and Vibration. 321, 2009, pp. 955–975.
4. Cebulski J.: Application of FeAl intermetallic phase matrix based alloys in the turbine components of a turbocharger. Metalurgija, vol. 54, iss. 1, 2015, pp. 154–156.
5. Cebulski J.: Żaroodporność stopów na osnowie fazy międzymetalicznej FeAl. Wydwnictwo Politechniki Śląskiej, Gliwice 2014.
6. Martinez-Botas R., Roamgnoli A.: Heat transfer analysis in a turbocharger turbine: An experimental and computational evaluation. Apllied Thermal Engineering, 38, 2012, pp. 58–77.
7. Jablońska M, Jasik A, Hanc A. Structure and some mechanical properties of Fe(3) Al-based cast alloys. Archives of Metallurgy and Materials. 54 (3), 2009, pp. 731–739.
8. Pint B.A., Haynes J.A., Armstrong B.L.: Performance turbocharger alloys and coatings at 850–950°C in air with water vapor. Surface & Coatings Technology, 215, 2013, pp. 90–95.
9. Shen p. Z., Song M., Gao H. Y., He Y. H., Zou J., Xu N. P., Huang B. Y., liu C. T.: Structural characteristics and high-temperature oxidation behavior of porous Fe-40% Al alloy. Journal of Materials Science, 44:4413, 2009.
10. Cebulski J., Pasek D.: Fe-Al Intermetallic Alloy: Its Heat-Resistant and Practical Application. Intermetallic Compounds – Formation and Applications. 2018.
11. Cebulski J.: Stopy na osnowie fazy międzymetalicznej FeAl. Monografia. Gliwice, 2020.
12. Cebulski J, Lalik S, Michalik R. Corrosion resistance of FeAl intermetallic phase based alloy in water solution of NaCl. Journal of Achievements in Materials and Manufacturing Engineering. 27, 2008, pp. 15–18.
13. Ślebioda T., Krawczyk J., Bednarek S., Wojtaszek M., Paćko M.: Chosen tribological properties of FeAl alloys. Tribologia, 42, nr 4, 2011, pp. 253–261.
14. Ślebioda T.: Thermomechanical processing of FeAl alloys. AGH, Kraków, 2013, pp. 73–78.
15. Górecka R., Polański Z.: Metrologia warstwy wierzchniej. Wydawnictwo WNT, 1987.
16. Gabryś D.: Analiza termodynamiczna układu turbodoładowania silnika spalinowego. Archiwum Instytutu Techniki Cieplnej, vol. 2, 2016, pp. 35–58.